Effect of Water on Zn Electrodeposition from a Deep Eutectic Solvent

Journal of The Electrochemical Society, 2024 **171** 012505

Effect of Water on Zn Electrodeposition from a Deep Eutectic Solvent

Abhishek Lahiri,[1,*,z] Pranay Hirani,[1] Sophia Haghani,[2] and Frank Endres[3]

[1]*Department of Chemical Engineering, Brunel University London, Uxbridge UB8 3PH, United Kingdom*
[2]*Experimental Techniques Centre, College of Engineering, Design and Physical Science, Brunel University London, Kingston Lane, London UB8 3PH, United Kingdom*
[3]*Institute of Electrochemistry, Clausthal University of Technology, Clausthal-Zellerfeld, 38678, Germany*

The electrodeposition of Zn films from a deep eutectic solvent (DES) of $ZnCl_2$ and formamide and its mixture with water was studied. From spectroscopic analyses it was observed that water up to 30 v/v% does not change the Zn coordination in the electrolyte after which significant change in the coordination was observed. Electrochemical studies showed that with increase in water concentration in the DES, higher deposition/stripping current was achieved which was related to lowering of viscosity. The Zn deposit morphology changed significantly with water concentration. At low concentrations of water (up to 20 v/v%), porous Zn nanoplates formed whereas the morphology changed to a dense hexagonal structure on increasing the water concentration. X-ray diffraction results confirmed that at low water concentrations (up to 20 v/v%) Zn-Cu alloy formed. Above 20 v/v% water concentration in the DES, Zn peaks evolved with Zn-Cu alloy forming a shoulder. Based on the electrochemical and spectroscopic studies, it appears that 20–30 v/v% water is the critical region wherein significant changes occur from a DES rich region to a water-rich region.

 [DOI: 10.1149/1945-7111/ad1d99]

Manuscript submitted October 3, 2023; revised manuscript received January 7, 2024. Published January 23, 2024.

Deep eutectic solvents (DES) are fast emerging as environmentally benign electrolytes for electroplating and energy storage devices. Their physicochemical and electrochemical properties can be tuned by changing the Lewis or Bronsted acids or bases components of the DES.[1–3] Compared to traditional aprotic ionic liquids, DES have the advantage of being cost-effective.[4] However, challenges remain regarding its smaller electrochemical window compared to aprotic ionic liquids which limits its application towards electrodeposition of various transitional metals, semiconductors and their alloys, and Li/Na.

Zn batteries are emerging as a fast-growing alternative to Li-ion batteries due to their inherent safety, non-toxicity, ease of handling and recyclability.[5–8] Although Zn can be electrodeposited from aqueous electrolytes, there are major impediments to overcome for use in Zn batteries such as formation of dendrites during deposition/stripping process, passivation of Zn electrodes and evaporation of the electrolyte.[6–8] In comparison, DES have shown to be a good medium for the deposition of Zn and has recently shown to be promising electrolytes for Zn-ion batteries.[9,10] Most DES for Zn deposition have been made from choline chloride (ChCl): Urea/glycerol/ethylene glycol eutectic mixtures containing Zn salts which has shown to inhibit dendrite formation during Zn deposition/stripping.[11–13] However, issues regarding high viscosity and low ionic conductivity need to be overcome as they affect the Zn diffusion process.

Recently, addition of water to DES or hydrated DES has been shown to change the physicochemical properties of the electrolyte.[14–18] Depending on the water concentration in DES, structural changes have been observed: Low water concentration (0%-15% w/w) has shown to change the 3D structure of the DES components which destroys the ion-clusters and the ion-pairs gets surrounded by water.[14] Subsequent water addition (50% w/w) leads to a weakening of the ion interaction in DES. However, the supramolecular structure is still preserved.[15–18] Further addition of water leads to disappearance of the molecular interaction in DES until it becomes an aqueous solution. Recent studies using inelastic neutron scattering spectroscopy showed that water does not behave uniformly and depends on the DES. Water was found to enhance the hydrogen bonds in ChCl:Urea whereas solvated DES was observed for ChCl:lactic acid.[19] These structural changes would inherently change the physicochemical and electrochemical properties of DES. Little has been looked into DES in the presence of water for metal deposition.[20] However, the effect of Zn speciation in the electrolyte and the change in speciation in presence of water and its relation to electrodeposition has not yet been investigated in detail. Understanding the correlation between Zn solvation, electrodeposition parameters and morphology is important for the use of DES based electrolytes in Zn electroplating with controlled morphology as well as for Zn based batteries where dendrite-free deposition is an important criterion.

The present study investigates the influence of varying concentrations of water in $ZnCl_2$-formamide (FA) (1:4 molar ratio) based DES using spectroscopic and electrochemical analyses to understand the influence of water on the solvation structure of DES and its influence on Zn electrodeposition. Formamide was selected for its notable polarity and high dielectric constant.[21]

Experimental

Formamide (99.5%), anhydrous $ZnCl_2$ (99.99%) and the copper substrates (99.9%) were purchased from Fisher Scientific. Zn (99.9%) was purchased from Pi-Kem. DES electrolyte was prepared by mixing $ZnCl_2$ in formamide at 1:4 molar ratio and heated at 70 °C for 3 h after which the solution was cooled to room temperature. Various concentrations of water (10%–80%, v/v) was added to the electrolyte and stirred for one hour before usage.

The cyclic voltammetry (CV) and electrodeposition experiments were carried out using a three-electrode cell setup with Cu as the working electrode and Zn as the counter and reference electrodes, respectively. The distance between the anode and cathode was about 5 mm. All the experiments were performed at 22 °C which was maintained in the laboratory. Prior to use, the Cu substrates were polished with Carbimet PSA 2000 from Beuhler for 10 min and subsequently cleaned in isopropanol and acetone by sonication. The CV and electrodeposition experiments (both potentiostatic and galvanostatic) were carried out using Biologic VSP-3e potentiostat/galvanostat. The FTIR and Raman spectra of the electrolyte were acquired using Shimadzu IRspirit and Renishaw inVia confocal Raman microscope, equipped with a 514 nm laser (Stellar-REN) and using a diffraction grating of 1800 lines/mm with a Renishaw CCD

*Electrochemical Society Member.
[z]E-mail: abhishek.lahiri@brunel.ac.uk

camera as the detector, respectively. For Raman, the samples were run with laser power at 100% using the 5× objective lens with a 532 nm laser, respectively. The viscosity of the electrolyte was evaluated using Rheosense microvisc and the contact angle was measured using Ossila contact angle goniometer.

Phase identification and structural analysis were performed using a Bruker D8 Advance X-ray diffractometer (XRD) fitted with a copper source, CuKα at a wavelength of $\lambda = 1.5406$ and a LynxEye^{TM} silicon strip detector. The patterns were recorded between $2\theta = 20°-80°$ in Bragg-Brentano mode with a step size of 0.01°. Morphological examinations were performed using a Zeiss Supra 35VP scanning electron microscope (SEM), at 20 kV operating voltage equipped with an EDAX Octane Super silicon drift EDX detector. The surface topography and root mean square roughness (RMS) of copper substrates were imaged in light tapping mode using a Dimension 3100 atomic force microscope (AFM) with Nanoscope IIIa controller (Digital Instruments, Santa Barbara, CA, USA). The RMS value for different polished copper surface was found to be between 72 and 81 nm. The scan rate was set to 1.0 Hz and 256 pixels per line to achieve good resolution of the surface topographical features.

Results

Figure 1 compares the IR and Raman spectra of addition of water to $ZnCl_2$:formamide (1:4) DES. From Fig. 1a it is evident that on addition of water the stretching peaks of CO, CN and δ_{CN} and δ_{HNH} upshift which is related to the water interacting with the DES.[22] Between 2500 and 4000 wavenumbers (Fig. 1b), the N-H peaks from formamide only show an increase in the intensity. Furthermore, an additional signal at 3570 cm^{-1} is observed on addition of water and with increase in water concentration, this signal upshifts and merges to form a shoulder. It is evident that until 30% of water addition, the signal is prominent after which a shoulder is formed. This indicates that the addition of water up to 30% remains bound to $ZnCl_2$:formamide after which some free water exists in the electrolyte. The Raman spectra of the DES with addition of water is shown in Fig. 1c. The peak at 1676 cm^{-1} relates to H-bonded formamide whereas the peak at 1584 cm^{-1} is due to NH_2 symmetric bending mode.[22] Both of these peaks upshift on addition of water. The peaks at 1339 and 1390 cm^{-1} are related to CN stretching modes. The addition of water results in lowering the intensity and wavenumbers in the spectra (Fig. 1d). The coordinated Zn-Cl stretching occurs at 286 cm^{-1} (Fig. 1c) which only shows a change in intensity on addition of water. Based on the changes in the CN stretching mode, it is possible to evaluate the coordination of Zn in the DES.[23] The coordination number can be estimated using Eq. 1 where $n_{FA\text{-}Zn}$ is the coordination number, I_i is the integrated intensity at 1339 cm^{-1} and Ji is the specific intensity of the band.[23]

$$n_{FA-Zn} = \frac{I_i}{C_{Zn} J_i} \quad [1]$$

Figure 2 shows the deconvoluted Raman spectra of the CN stretching with different concentrations of water added to the DES with a Voigt function. The bands deconvoluted at 1309 (red curve) and 1339 cm^{-1} (green curve) relates with FA and Zn coordinated with FA, respectively, whereas the peak at 1379 and 1391 cm^{-1} are related to Zn coordinated FA (blue curve) and δ_{FA} (cyan curve), respectively.[23] Using Eq. 1, the coordination number for

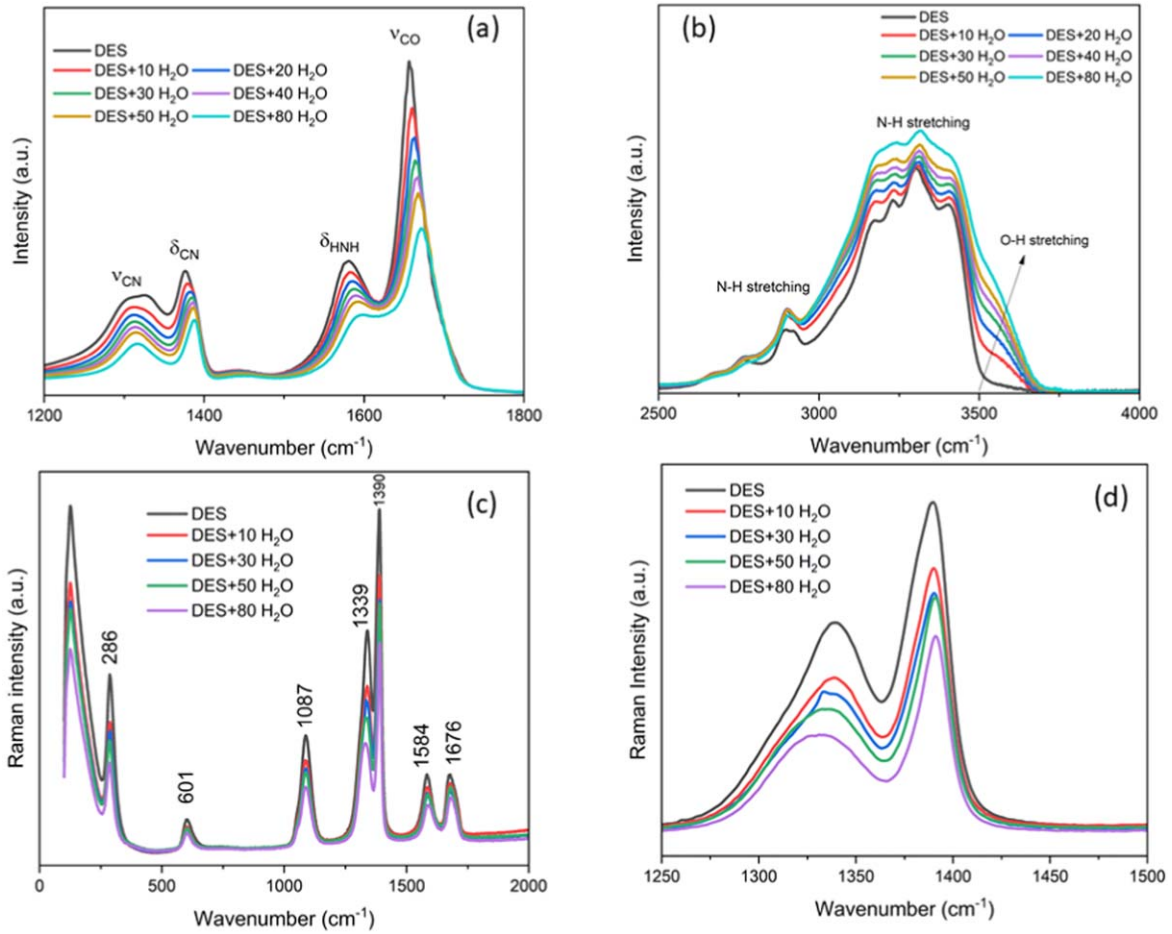

Figure 1. IR spectra of DES with different concentrations of water (a) between 1200 and 1800 cm^{-1} (b) between 2500 and 4000 cm^{-1} (c) Raman spectra of DES with different concentrations of water (d) Raman spectra of CN starching region of DES with different concentrations of water.

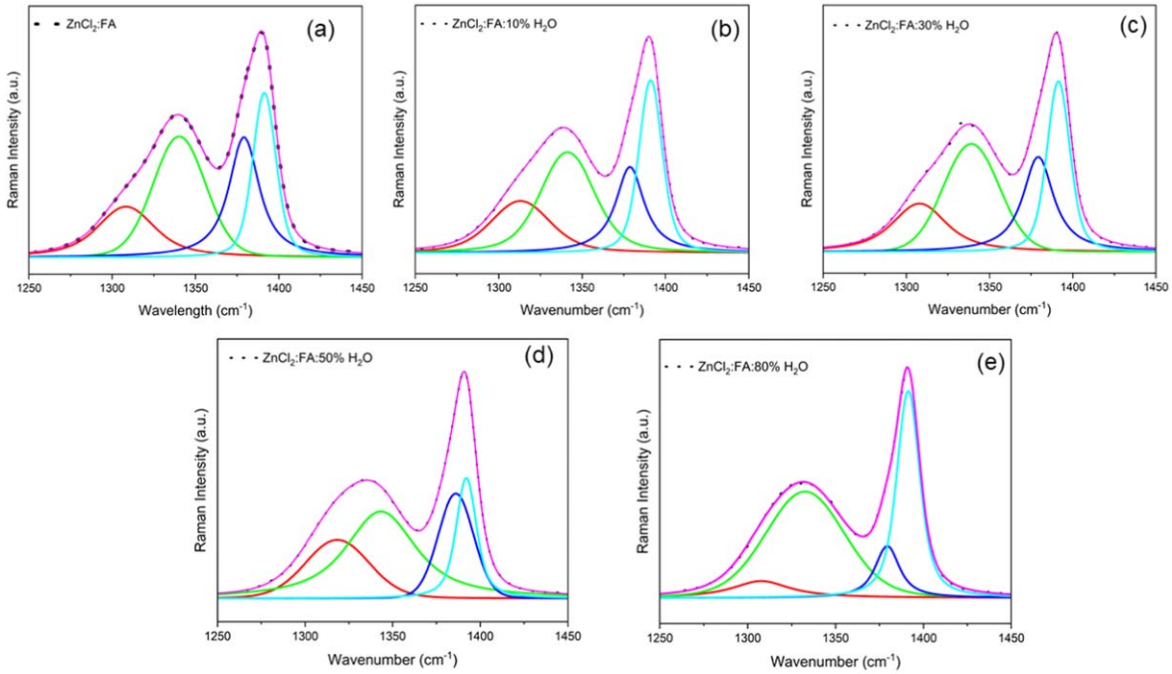

Figure 2. The Raman spectra deconvoluted using Voigt fit for (a) $ZnCl_2$:FA (b) $ZnCl_2$:FA with 10 v/v% water (c) $ZnCl_2$:FA with 30 v/v% water (d) $ZnCl_2$:FA with 50 v/v% water (e) $ZnCl_2$:FA with 80 v/v% water.

$ZnCl_2$:Formamide was found to be 4 using the values obtained from 1309 and 1339 cm^{-1}, suggesting the formation of $ZnCl_4^{2-}$. However, $ZnCl_4^{2-}$ should lead to the Raman peak at 275 cm^{-1},[24,25] whereas the peak obtained in the Raman spectra is at 286 cm^{-1} suggesting the formation of $ZnCl_3^-$.[26] Therefore, it appears that the possible Zn species in the DES is $[ZnCl_3FA]^-$ and $[ZnClFA]^+$. In comparison to FA, the DES with acetamide had shown the formation of $[ZnCl(acetamide)]^+$, $[ZnCl(acetamide)_2]^+$ and $[ZnCl(acetamide)_3]^+$ which was evaluated using mass spectroscopy.[27] The difference in the speciation might be due to the high dielectric constant of FA.

The addition of 10% and 30% water to the DES did not change the coordination number. However, with the addition of 50% and 80% water (Figs. 2d and 2e), the calculation with Eq. 1 led to an error in coordination number. This suggests that addition of water up to 30% is bound to the DES and does not affect the $ZnCl_2$:FA coordination, whereas on higher water concentrations, this coordination is broken. This is further supported by the IR spectra wherein a peak is observed until 30% water after which a shoulder is formed suggesting that until 30% the water remains bound after which there is free water which possibly interacts with $ZnCl_2$ finally resulting in partial collapse of $[ZnCl_3FA]^{2-}$ structure.

Cyclic voltammetry was used to evaluate the electrochemical behaviour of various DES electrolytes. Figure 3 shows the CV curves of DES with various concentrations of water. In DES (Fig. 3a, on scanning in the negative potential regime, a shallow peak C* is observed in the negative potential which is related to Cu-Zn alloy formation. The inset in Fig. 3a shows the derivative of the cathodic curve which clearly shows the formation of Cu-Zn alloy peaking at 0 V. The alloy peak is followed by a sharp increase in negative current below 0 V which corresponds to the deposition of Zn. In the anodic regime, an oxidation peak at 0.15 V is observed which is followed by another peak at 0.28 V. The peak at 0.15 is due to dissolution of Zn and the peak at 0.28 V relates to dissolution of Cu-Zn alloy.[28] On addition of 30% water, again Zn deposition is observed with a much higher current at 0 V compared to the pure DES, Fig. 3a. In the anodic scan, a dominant peak at 0.15 V is observed and the second peak at 0.28 V almost disappears. With increase in water concentration in the DES (Figs. 3c and 3d, it is evident that both the Zn deposition (commencing at 0 V) and the dissolution current (0.15 V) increase whereas the second oxidation peak disappears. The loss in the second oxidation peak with higher water concentration indicates more Zn is deposited which inhibits the oxidation/dissolution of the Cu-Zn alloy.

The increase in deposition/stripping current can be related to decrease in viscosity of the electrolyte as measured and shown in Fig. 4a. The viscosity of $ZnCl_2$:FA was found to be 227 mPa s at 21 °C which is comparable to $ZnCl_2$ based DES with acetamide, ethylene glycol and 1-butylpyrrolidine.[27,29] With increase in water concentration in the DES electrolyte, the viscosity decreased exponentially and almost plateaued above 30% water concentration. Besides viscosity, the contact angle at the solid-liquid interface is of great importance as it delivers information on the interfacial surface energy, the wettability and the electrochemical properties of the interfaces.[30–32] The influence of water on the contact angle was thus measured.

DES showed a high contact angle of 77° on copper which decreases slightly on addition of water up to 30%. The contact angle on addition of 30% water was found to be 64°. However, further addition of water was found to increase the contact angle again. The lowest contact angle was measured when 80% water was added. The contact angle measurements indicate that at 30% water concentration in the DES, the electrode/electrolyte interface changes significantly which must affect the electrodeposition process. As the roughness of the copper substrate used was almost same, the changes in the contact angle might be due to change in the Zn solvation in the electrolyte and its interaction with the Cu. Water has shown to affect the solid-liquid interface at a similar concentration (20–30 v/v%) on using aprotic ionic liquids.[33]

In order to understand the effect of viscosity and wettability on electrodeposition, Zn was deposited from different DES-water electrolytes. Figure 5 compares the microstructure of Zn electrodeposited on copper at −0.1 V. It is evident that from DES and with addition of 10% water in DES, a porous Zn deposit is observed. On addition of 20% water, interestingly, the morphology changes and Zn particles are observed having particles size of about 1 μm.

With the addition of 30% water and above in the DES, a hexagonal faceted Zn deposit is evident which covers the entire

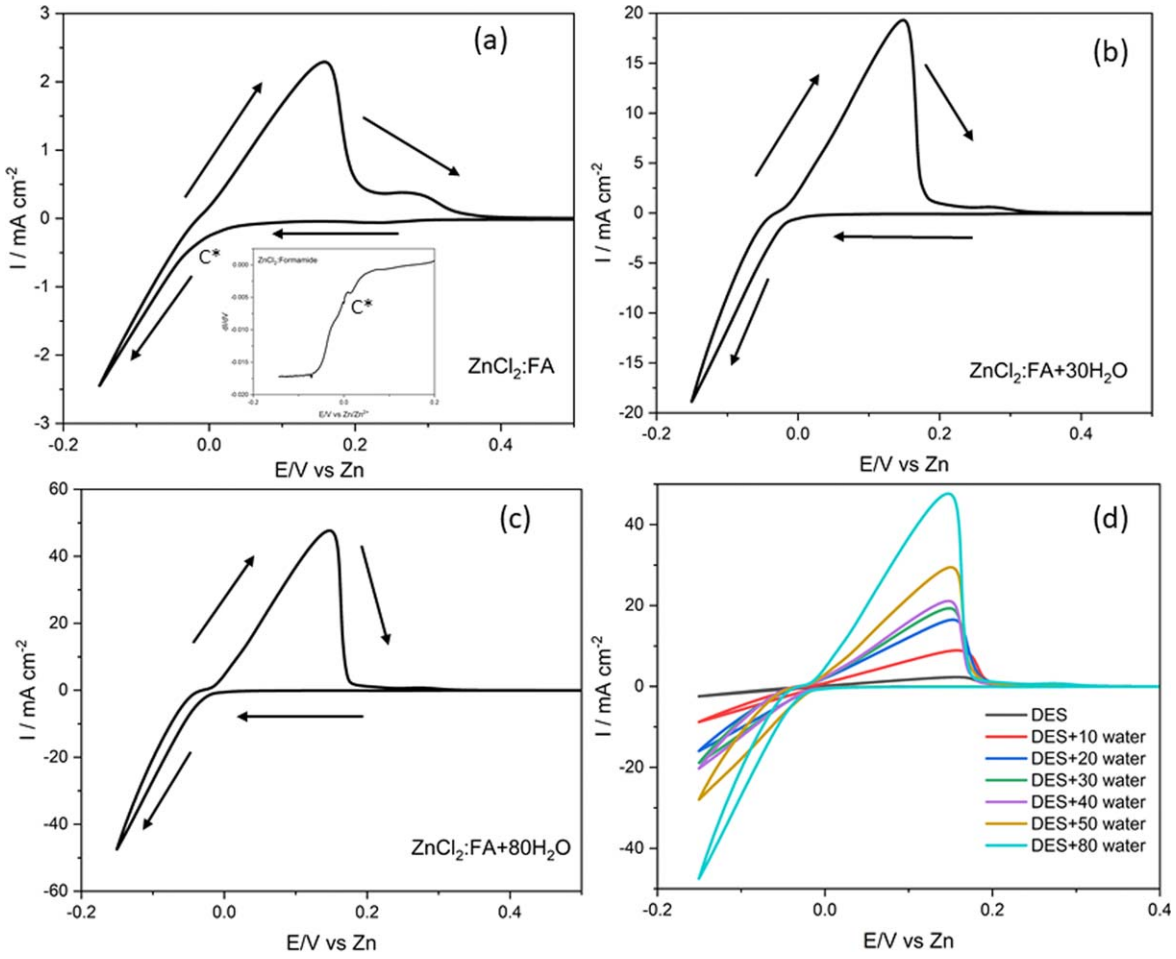

Figure 3. CV of (a) $ZnCl_2$:FA (The inset shows the derivative of the negative regime of the CV curve) (b) $ZnCl_2$:FA+10 v/v% water (c) $ZnCl_2$:FA+v/v30% water (d) $ZnCl_2$:FA+80 v/v% water at room temperature on copper.

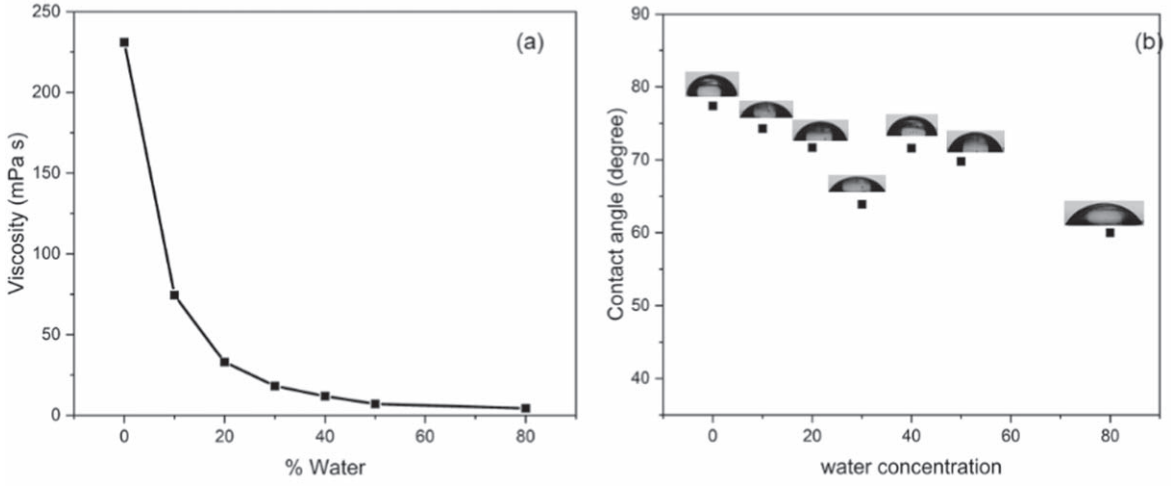

Figure 4. (a) Change in viscosity of DES with addition of water measured at 21 °C (b) Change in the contact angle of DES on copper with addition of water.

surface of copper. XRD was used to confirm the Zn deposit. Figure 6a compares the XRD of the Zn deposits on copper substrates from three different electrolytes. It is evident that besides the Cu (200) peak, peaks at 43° and 54.8° are observed which relate to Zn peaks and are in agreement with Zn ICDD data (78–9363). The expanded region between 42° and 44° is shown in Fig. 6b from which it is evident that with increase in water concentration, peak broadening and a peak shift takes place.

For DES the peak at 43.3° relates to the formation of Cu-Zn alloy (ICDD 71–7928) and on addition of 10 v/v% water a peak broadening takes place with the formation of a shoulder at 43.1° which relates to formation of Zn. With 20 v/v% water addition, a dominant peak at 43.1° and a shoulder at 43.3° are observed. On further increase in water concentration in DES (50 v/v% water), the peak shifts to 43.1°. Based on the XRD, it is evident that the addition of water improves the Zn deposition. Similar studies with the addition

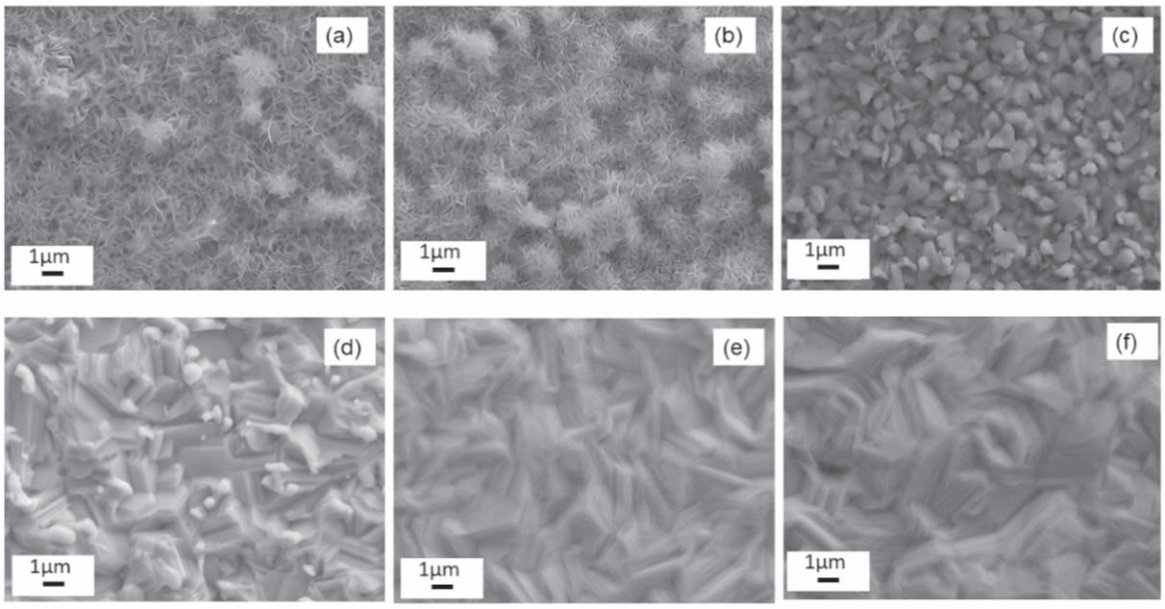

Figure 5. Microstructure of Zn deposited from (a) DES (b) DES+10%water (c) DES+20% water (d) DES+30%water (e) DES +40% water (f) DES+80% water.

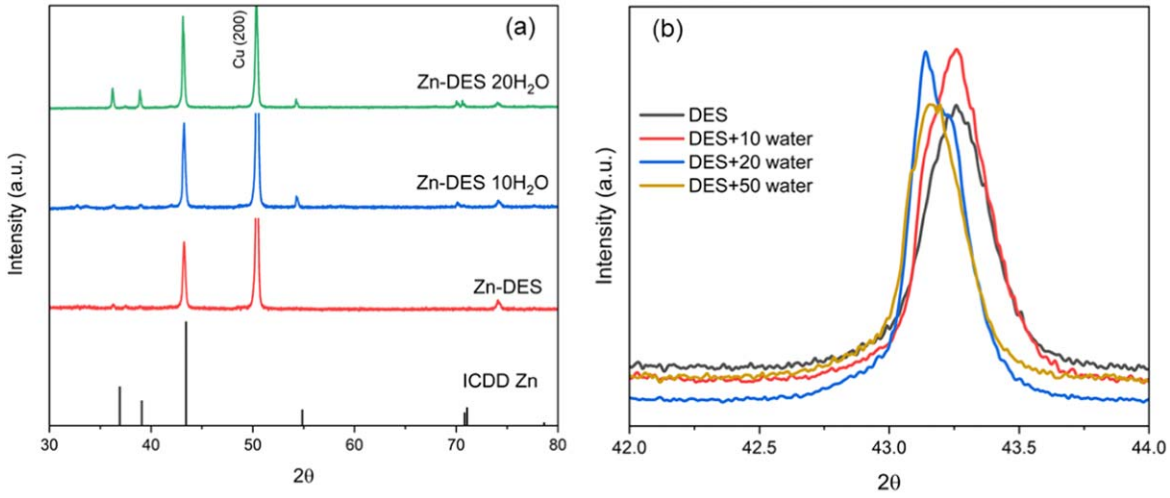

Figure 6. (a) Comparison of XRD of Zn deposited on copper from different electrolytes (b) XRD between 42 and 44° of Zn deposit from different DES electrolytes.

of organic solvents to $ZnCl_2$ containing ionic liquids showed similar behaviour wherein the addition of organic solvents improved the electrodeposit and led to a change in morphology.[34] In ChCl based deep eutectic solvent, organic additives affected the morphology of Zn deposit.[11] In our study, the addition of water reduces the environmental concerns related to Zn electrodeposition. Thus, based on SEM and XRD results, it is evident that with lower water concentration, Cu-Zn alloy is the dominant phase which results in the formation of porous Cu-Zn deposit (Figs. 5a and 5b) whereas increase in water concentration above 20 v/v% leads to formation of thick Zn deposit resulting in hexagonal facets as observed in Figs. 5c –5e.

Galvanostatic deposition was also carried out to understand the change in Zn morphology and Zn phases on copper. Figure 7 shows the Zn deposition when a current density of 1 mA cm^{-2} was applied for 1 hour. From the microstructure it is evident that Zn deposit from DES and DES-water mixture electrolytes result in relatively uniform Zn particles with size ranging from 0.5 to 1 μm. However, on addition of 20 and 40 v/v% water, besides irregular morphology porous Zn structures are also observed.

Figure 8 compares the XRD of Zn deposited galvanostatically. It is evident from Fig. 8a that besides Cu (200) which occurs at 50°, all the other peaks relate to Zn. To distinguish Zn and Zn-Cu alloy formation, the XRD peak between 42° and 44° are shown in Fig. 8b. It is evident that Zn deposited from DES and DES with 10% water shows the formation of Zn-Cu alloy whereas Zn deposits are observed on increasing the water concentration as the peak shifts negatively as observed previously for Zn deposited potentiostatically in Fig. 6.

Furthermore, a shoulder is also observed at 43^{o} with a main peak arising at 43.2^{o}. The peak split might be due to Zn and different Zn-Cu alloy compositions.[35] Thus, comparing the XRD of both galvanostatic and potentiostatic deposition, it is evident that above 30 v/v% water in $ZnCl_2$-formamide DES leads to thick Zn plating.

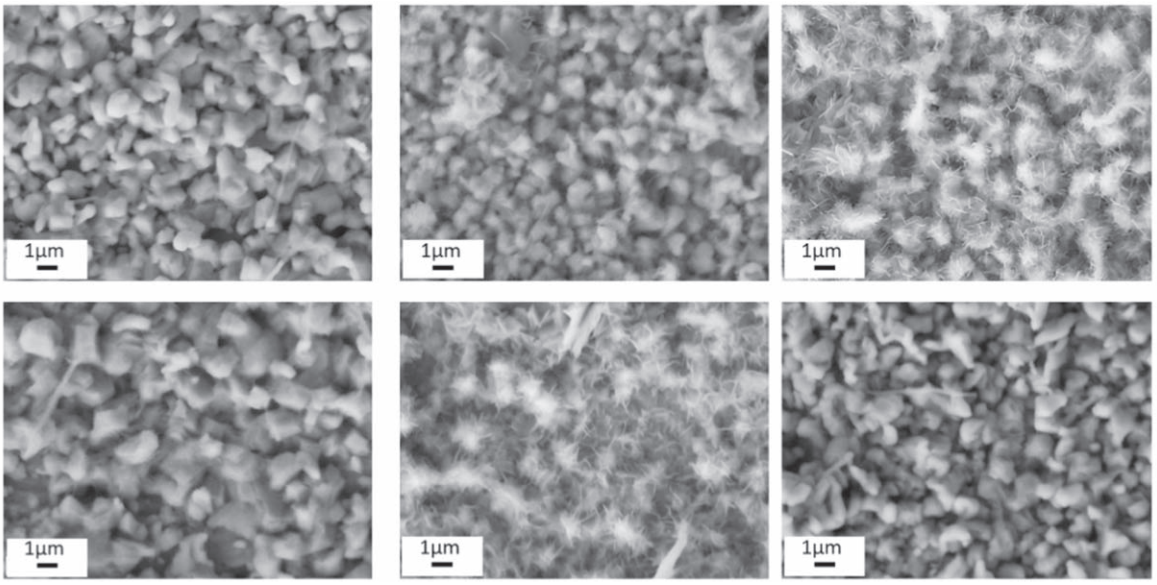

Figure 7. Microstructure of Zn deposited from (a) DES (b) DES+10 v/v% water (c) DES+20 v/v% water (d) DES+30 v/v% water (d) DES +40 v/v% water (e) DES+80 v/v% water.

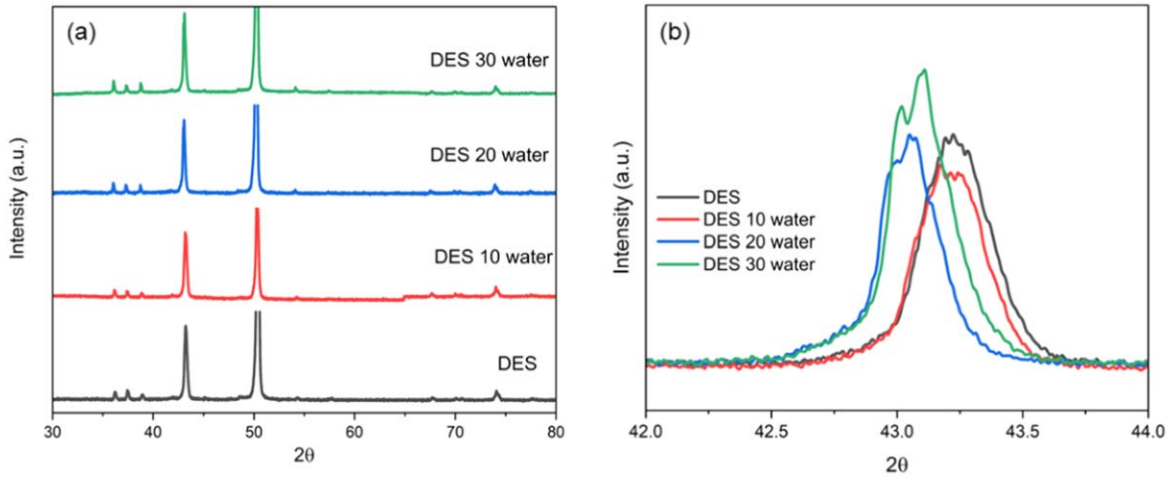

Figure 8. (a) Comparison of XRD of Zn deposited on copper from different electrolytes at a constant current density of 1 mA cm^{-2} for 1 hour (b) XRD between 42 and 44° of Zn deposit from different DES electrolytes.

Conclusions

In this paper we have shown the influence of water in a DES for Zn electrodeposition on copper. It was observed that water does not change the Zn solvation until 30 v/v% after which significant changes in the Zn solvation takes place. The change in solvation leads to a change in surface wetting, thereby changing the CV. The CV results showed that the increase in water increases the deposition/stripping current. From potentiostatic deposition of Zn on copper, a clear change in Zn deposit morphology could be observed on changing the water concentration from 20 to 30 v/v%. However, galvanostatic deposition did not show a significant change in Zn morphology with the addition of water. From XRD analysis, it was observed that with low water concentration in the electrolyte, Zn-Cu alloy dominated the deposit whereas with increase in water clear Zn deposit peaks were observed.

Acknowledgments

This research was funded, in whole by EPSRC, EP/W015129/1. We would also thank Dr Myles Worsley for help with Raman spectroscopy.

Data Availability Statement

Data have been made available in Brunel University London's repository via Brunel Figshare database.

ORCID

Abhishek Lahiri https://orcid.org/0000-0001-8264-9169
Frank Endres https://orcid.org/0000-0002-5719-7241

References

1. B. B. Hansen et al., *Chem. Rev.*, **121**, 1232 (2021).
2. E. L. Smith, A. P. Abbott, and K. S. Ryder, *Chem. Rev.*, **114**, 11060 (2014).
3. K. A. Omar and R. Sadeghi, *J. Mol. Liq.*, **360**, 119524 (2022).
4. A. Paiva, R. Craveiro, M. Martins, R. L. Reis, A. R. C. Duarte, and A. C. S. Sustainable, *ACS Sustainable Chem. Eng.*, **2**, 1063 (2014).
5. L. E. Blanc, D. Kundu, and L. F. Nazar, *Joule*, **4**, 771 (2020).
6. Z. Ye, Z. Cao, M. O. L. Chee, P. Dong, P. M. Ajayan, J. Shen, and M. Ye, *Energy Storage Mater.*, **32**, 290 (2020).
7. T. Zhao, N. Zhang, C. Wu, and Y. Xie, *Energy Environ. Sci.*, **13**, 1132 (2020).
8. S. Mallick and C. R. Raj, *Chem. Sus. Chem*, **14**, 1987 (2021).
9. X. Ji, *eScience*, **1**, 99 (2021).
10. M. E. Di Pietro and A. Mele, *J. Mol. Liquids*, **338**, 116597 (2021).
11. A. P. Abbott, J. C. Barron, G. Frisch, K. S. Ryder, and A. F. Silva, *Electrochim. Acta*, **56**, 5272 (2011).

12. W. Kao-ian, R. Pornprasertsuk, P. Thamyongkit, T. Maiyalagan, and S. Kheawhom, *J. Electrochem. Soc.*, **166**, A1063 (2019).
13. M. Han, J. Huang, X. Xie, T. C. Li, J. Huang, S. Liang, and J. Zhou, *Adv. Funct. Mater*, **32**, 2110957 (2022).
14. C. Ma, A. Laaksonen, C. Liu, X. Lu, and X. Ji, *Chem. Soc. Rev.*, **47**, 8685 (2018).
15. F. Gabriele, M. Chiarini, R. Germani, M. Tiecco, and N. Spreti, *J. Mol. Liq.*, **291**, 111301 (2019).
16. D. Shah and F. S. Mjalli, *Phys. Chem. Chem. Phys.*, **16**, 23900 (2014).
17. O. S. Hammond, D. T. Bowron, and K. J. Edler, *Angew. Chem. Int. Ed.*, **56**, 9782 (2017).
18. Y. Dai, G.-J. Witkamp, R. Verpoorte, and Y. H. Choi, *Food Chem.*, **187**, 14 (2015).
19. M. M. Nolasco et al., *Front. Phys.*, **10**, 834571 (2022).
20. E. Emanuele, A. Li Bassi, A. Macrelli, C. Mele, J. Strada, and B. Bozzini, *Molecules*, **28**, 957 (2023).
21. J. R. Reimers and L. E. Hall, *J. Am. Chem. Soc.*, **121**, 3730 (1999).
22. K. Ohasi, N. Hikiishi, and H. Takeshita, *Spectrochim. Acta A Mol Biomol Spectrosc*, **206**, 112 (2019).
23. L. M. Pereira and W. A. Alves, *Vib. Spectrosc.*, **56**, 250 (2011).
24. N. Trendafilova, G. S. Nikolov, R. Kellner, and G. Bauer, *Vib.Spectrosc.*, **6**, 351 (1994).
25. M. Scrocco, *Spectrochim.Acta, Part A*, **33**, 357 (1977).
26. D. F. C. Morris, E. L. Shortand, and D. N. Waters, *J. Inorg. Nucl. Chem.*, **25**, 975 (1963).
27. A. P. Abbott, J. C. Barron, K. S. Ryder, and D. Wilson, *Chem Euro J.*, **13**, 6495 (2007).
28. S. Xu, Y. Zhu, D. Xiong, L. Wang, P. Yang, and P. K. Chu, *J. Phys. Chem. C*, **121**, 3938 (2017).
29. G. Pulletikurthi, M. S. Ghazvini, T. Cui, N. Borisenko, T. Carstens, A. Borodin, and F. Endres, *Dalton Trans.*, **46**, 455 (2017).
30. F. Endres, *Phys. Chem. Chem. Phys.*, **14**, 5008 (2012).
31. M. Tariq, M. G. Freire, B. Saramago, J. A. P. Coutinho, J. N. C. Lopes, and L. P. N. Rebelo, *Chem. Soc. Rev.*, **41**, 829 (2012).
32. W. Wang and R. W. Murray, *Anal. Chem.*, **79**, 1213 (2007).
33. T. Cui, A. Lahiri, T. Carstens, N. Borisenko, G. Pulletikurthi, C. Kuhl, and F. Endres, *J. Phys. Chem. C*, **120**, 9341 (2016).
34. Y.-F. Lin and I. Wen Sun, *Electrochim. Acta*, **44**, 2771 (1999).
35. R. Juškėnas, V. Karpavičienė, V. Pakštas, A. Selskis, and V. Kapočius, *J. Electronanal. Chem.*, **602**, 237 (2007).